32nd IFSCC Congress
London 19-22 September 2022

Poster ID 450

Wound Healing and Skin Regeneration on FT-skin

Marisa Meloni[1], Bernadette Lombardi[2], Francesco Carriero[1], Laura Ceriotti[1]
[1]VitroScreen Srl, Milan, Italy, [2]Telethon Institute of Genetics and Medicine (TIGEM), Pozzuoli, Italy

VitroScreen
Leading Innovation in Pre-Clinical Testing

Introduction

Skin regeneration is a physiological and complex process involving different cell types to restore tissue continuity after wound: activated keratinocytes migrate from the wound edges to generate a provisional wound bed matrix where they can proliferate, differentiate, and stratify into a new epidermis. The complete skin repair process involves fibroblasts activation and ECM remodelling.

The aim of this research work was to develop an *in vitro* experimental model on a commercially available 3D reconstructed Full Thickness skin (FT-skin) to recapitulate skin regeneration dynamic over time highlighting the involved cell machineries.

The wound healing preclinical model described in this work has been further developed by VitroScreen within the project EUROSTARS E! 113238 aimed at developing a new model that takes into account *S. aureus* infecting diabetic wounds.

Materials & Methods

Phenion® Full Thickness Skin Models produced by Henkel (Düsseldorf, Germany, diameter of 1.4cm and surface area of 1.5cm^2) are cultured from keratinocytes and dermal fibroblasts derived from biopsy material from a single healthy donor to form a multi-layered skin equivalent that resembles human skin under culture conditions. The FT-skin tissues were injured at both epidermal and dermal level with a sterile 1 mm biopsy punch (Fig. 1) and subsequently cultured for up to 20 days.

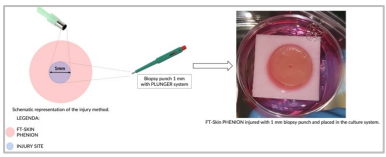

Fig. 1 Schematic representation of injury procedure in a FT-Skin model. One single injury is performed with a 1-mm biopsy punch with plugger in the centre of each FT-skin model to create a physical discontinuity in both epidermis and dermis layers and induce a redistribution of fibroblasts in the wound bed.

At defined time-points (**0, 3, 8 and 20 days**), FT-skin tissues were fixed in 10% buffered formalin (Sigma Aldrich, HT501128) and embedded into paraffin blocks: sections of 5 µm were obtained. Slides were stained with Haematoxylin and Eosin (H&E) and immunolabeled (IHC/IF) with biomarkers reported in Table I.

Table I. Primary antibodies list

Protein target	Primary Ab Code	Supplier
Hyaluronic acid (HA)	AMS.HKD-BC41	AMSBio
Collagen I (COL I)	ab88147	Abcam
Smooth muscle actin (α-SMA)	ab7817	Abcam
Fibronectin (FN)	ab2413	Abcam

All secondary antibodies were diluted 1:400 in PBS 1x. DAPI was used for nuclei staining. Images acquisition was performed by LEICA DMi8 THUNDER imager 3D System (Leica) composed by camera sCMOS K5 and LASX software 3.7.5.

Results & Discussion

Repair dynamics of tissues were investigated by H&E staining (Fig. 2) from day 0 to day 20.

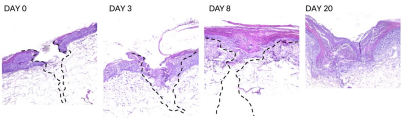

Fig 2. H&E staining shows morphological variation and progressive closure of wounds from day 0 up to day 20 from injury. Magnification 10X. Scale bar: 100 µm.

The epidermis seamlessly attached to the dermis compartment except in the wound area on day 0, providing an *in vivo*–like matrix for re-epithelialization surrounded by clearly defined wound margins. Tissue continuity is destroyed in both epithelial and dermal compartment. The extending epidermal tongue is visible as 1-2 cell layers in the wound bed on day 3: the presence of cells randomly distributed in the wound bed suggests the formation of new tissue. The keratinocytes covered 100% of the wound area on day 8 by organizing the epithelium into approximately three cell layers near the wound edges and one cell layer in the centre of the wound bed. The dotted line indicates the boundary between epithelium and dermis: keratinocytes are still visible repopulating in the wound bed. On day 20 it is possible to appreciate the dermal remodelling.

Nuclear shape and orientation in wounded and unwounded (negative control, NC) tissues were analysed during the repairing process in the wound bed (Fig. 3). FT-Skins were divided into three regions according to the wound gap position (wound bed, right edges and left edges) and the orientation of the major axis of the nuclei of the basal cells in the epidermis was quantified.

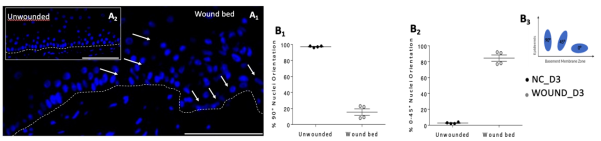

Fig. 3. Nuclei orientation in the unwounded tissue (NC)(A2, B1,2) and in the wound bed (A1, B1,2) on day 3. White arrows indicate nuclei deformation. Dotted lines indicate dermal-epidermal junction. A Cartesian reference system was used where the X axis corresponds to the basal membrane (B3). Magnification 40X. Scale bar: 100 µm.

On day 3 from the injury, a distribution that significantly differed from rotation angles of nuclei in unwounded tissues has been observed in regions of wounded skin. In particular, unwounded tissues show a distribution of nuclear orientations with a tendency towards 90° (B1) while wounded tissues towards 0-45° (B2) when considering a Cartesian reference system where the X axis corresponds to the basal membrane (B3). This data underline the establishment of the migratory phase.

The **activation of fibroblasts** in the injured tissue was studied by immunofluorescence (Fig. 4) and the number of a-SMA-positive cells compared to the total number of nuclei visible in the newly formed tissue was quantified (Tab II).

The FN expression was instead calculated in pixels as an integrated density area in the wound bed and edges.

The results of signal quantification at day 3 and day 8 are summarized in Tab II.

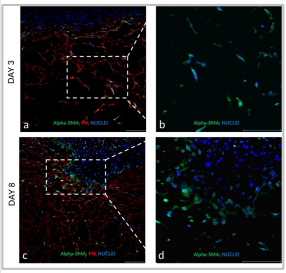

Fig. 4. IF of a-SMA and FN. Representative fluorescent images of α-SMA (green) and FN (green) double staining in the newly formed tissue of the wounded bed on day 3 (a - b) and day 8 (c - d). The red squares in a and c highlight fibroblasts activation in the dermis wound bed as visible in b and d for α-SMA on day 3 and day 8. Magnification 20X and 40X. Scale bar: 100 µm.

Table II. Quantification of a-SMA- positive cells and FN expression.

	DAY 3	DAY 8
α-SMA cells/N° tot cells	30%	35%
FN integrated pixels density	1,11 E+06	4,19 E+07

According to Fig. 4 results, α-SMA-positive fibroblasts (myofibroblasts) are randomly identified on day 3 (A and B). On day 8 (C and D), myofibroblasts are mainly located around the tongue of the newly formed epidermis. Moreover, in the wound area, FN expression levels increase around myofibroblasts (C): spotted signal of α-SMA positive fibroblasts corresponds to a strong red signal in the region of the wound. The quantitative analysis of myofibroblasts and FN expression (Tab II) confirm the activation of fibroblasts after the injury and their major role in the ECM remodelling process.

Dermal compartment regeneration was addressed by investigating the expression of HA and COL I as represented in Fig. 5 and quantified as reported in Tab. III.

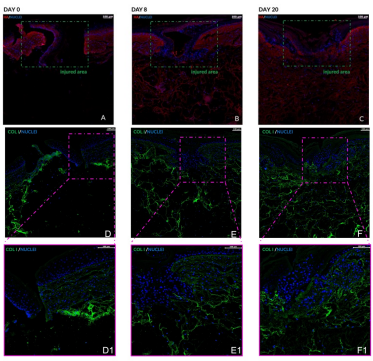

Fig. 5 IF of Hyaluronic acid (HA) and Collagen I (COL I) at day 0 (A, D and D1), day 8 (B, E and E1) and day 20 (C, F and F1) respectively. The figure includes representative fluorescent images of HABP and COL I in the newly formed tissue of the wounded bed. Magnification 10X and 20X. Scale bar: 100 µm.

Table III. Quantification of COL I and HA in the wound area, evaluated taking into account the intensity of the fluorescent signal.

	COL I	HA
DAY 0	Basal expression	Basal expression
DAY 8	+	++
DAY 20	++	++

At day 0, baseline expression of COL I and HA is visible in the extracellular matrix. Starting from day 8, in the wound bed, fibroblasts increase the synthesis and deposition of COL I and HA: this physiological mechanism is necessary, during the proliferative phase, to form the granulation tissue that acts as substrate for the epithelial cells migration. From day 8 to day 20, COL I significantly increases (images E & E1, F & F1) while HA is found stabile (images B and C).

HA, together with FN, is the main components that create a truly hydrated matrix and facilitate cell migration during the proliferative phase. In the final steps of skin regeneration HA is replaced by collagens: for this reason, the deposition of HA does not increase over time and it remains stable (Table III) whereas the Collagen I appears highly expressed.

As reported in the Literature, during the remodelling phase, a continuous synthesis and breakdown of collagen in the extracellular matrix is visible: collagen fibers are reorganized, cross-linked and aligned along lines of tension.

In the final stage of proliferative phase and during the transition from proliferative to remodelling phase, the deposition of COL I by fibroblasts increases in order to replace FN, HA and other proteoglycans of granulation tissues.

Conclusions

The experimental model developed on FT-skin recapitulates in a reduced time course the fundamental steps of skin regeneration process in the two skin compartments: it is a relevant, robust, reproducible preclinical *in vitro* model to investigate the skin regeneration properties of topically or systemically applied ingredients and formulations mirroring real life exposures and doses.

Furthermore, it allows a mechanistic approach to the assessment of efficacy of the ingredients at molecular level in particular in the dermal compartment: to investigate the proteins involved in ECM remodelling and address myofibroblasts features, which are confirmed as main actors in tissue granulation and wound contraction and as key target to counteract impaired skin repair or excessive fibrosis.

References:

Holly N. Wilkinson and Matthew J. Hardman (2020), Wound healing: cellular mechanisms and pathological outcomes, Open Biology, DOI: 10.1098/rsob.200223; T Velnar, T Bailey and V Smrkolj (2009), The Wound Healing Process: An Overview of the Cellular and Molecular Mechanisms, Journal of International Medical Research 2009 37: 1528 DOI: 10.1177/147323000903700531 ; Ellie A Lemaster (2013), Role of fibronectin in normal wound healing, International Wound Journal ISSN 1742-4801, doi: 10.1111/iwj.12109 ; Lombardi B, Casale C, Imparato G, Urciuolo F, and Netti PA (2017) Spatiotemporal Evolution of the Wound Repairing Process in a 3D Human Dermis Equivalent Adv. Healthc. Mater. 6(13):1–11.